Lindane degradation by electrooxidation process: Effect of electrode materials on oxidation and mineralization kinetics

Carmen M. Dominguez[1,2,*], Nihal Oturan[2], Arturo Romero[1], Aurora Santos[1], Mehmet A. Oturan[2,*]

[1] Dpto. Ingeniería Química, Facultad de Ciencias Químicas, Universidad Complutense Madrid. Ciudad Universitaria S/N. 28040, Madrid, Spain

[2] Université Paris-Est, Laboratoire Géomatériaux et Environnement, EA 4508, UPEM, 5 Bd Descartes, 77454 Marne-la-Vallée Cedex 2, France

Paper submitted to "*Water Research*" for consideration

*** Corresponding authors' Emails:**

carmdomi@ucm.es (Carmen M. Dominguez)

mehmet.oturan@univ-paris-est.fr (Mehmet A. Oturan)

Abstract

This study focuses on the effect of electrode materials on abatement of lindane (an organochlorine pesticide) by electrooxidation process. Comparative performances of different anodic (platinum (Pt), dimensionally stable anode (DSA) and boron-doped diamond (BDD)) and cathodic (carbon sponge (CS), carbon felt (CF) and stainless steel (SS)) materials on lindane electrooxidation and mineralization were investigated. Special attention was paid to determine the role of chlorine active species during the electrooxidation process. The results showed that better performances were obtained when using a BDD anode and CF cathode cell. The influence of the current density was assessed to optimize the oxidation of lindane and the mineralization of its aqueous solution. A quick (10 min) and complete oxidation of 10 mg L^{-1} lindane solution and relatively high mineralization degree (80% TOC removal) at 4 h electrolysis were achieved at 8.33 mA cm^{-2} current density. Lindane was quickly oxidized by *in-situ* generated hydroxyl radicals, (M(•OH)), formed from oxidation of water on the anode (M) surface following *pseudo* first-order reaction kinetics. Formation of chlorinated and hydroxylated intermediates and carboxylic acids during the treatment were identified and a plausible mineralization pathway of lindane by hydroxyl radicals was proposed.

Key Words: Lindane; Electrooxidation; Hydroxyl radicals; BDD; Carbon felt

1. Introduction

Organochlorine pesticides (OCPs) represent a major source of emerging water pollutants in recent decades (Usman et al., 2014; Khan et al., 2017a). Among the OCPs, lindane, the gamma isomer of hexachlorocyclohexane (γ-HCH), was widely used as a broad spectrum insecticide in agriculture and for public health purposes since the Second World War until the 1990s (Wang et al., 2009; Chang et al., 2011). As a result of its intense use, lindane residues (a mixture of α, β, γ, δ, and ε-HCH isomers) have been detected worldwide, ultimately entering into the human body through food chains (Behrooz et al., 2009). The HCHs isomers are among the most ubiquitous organochlorine pesticides and are easily found in the environment. They can be detected in real samples in a quite broad range: from ng L^{-1} in natural water (World Health Organization, 2004) to near its maximum solubility in water (10 mg L^{-1}) when polluted water comes directly from the washing of the solid product (HCH residues were often stockpiled in open piles) or by the dissolution of dense non-aqueous phase liquid (DNAPL) of these compounds. These pesticides are also bioaccumulative and can enter the food chain to reach and accumulate in human and animal tissues. As a consequence of its high toxicity and long persistence, lindane presents potential health risks to humans (skin irritation, dizziness, headaches, diarrhea, nausea, vomiting, convulsions, and even death) and animals (Heusinkveld et al., 2010). It was reported to be neurotoxic, a potential carcinogen and teratogen by the Environmental Protection Agency (EPA) and the World Health Organization (WHO) (Joo and Zhao, 2008). Therefore the concern for these pollutants has grown exponentially in recent years, resulting finally in lindane inclusion (along with α- and β-HCH) in the list of persistent organic pollutants (POPs) in the Stockholm Convention of 2009 (Vijgen et al., 2011). The use of lindane has been restricted in many European countries as well as in the

United States and Canada but it is still being used elsewhere (Khan et al., 2017a) and many landfills and other sites remain polluted by these compounds (Dutchak et al., 2004; Yang et al., 2010; Chang et al., 2011). Therefore, finding a solution for lindane decontamination has become a priority for the scientific community in recent years.

Several methods, including conventional techniques such as incineration (Peng et al., 2015), biological treatments (Camacho-Pérez et al., 2012), chemical oxidation (Usman et al., 2014) and reduction (Dominguez et al., 2016) have been used for lindane degradation in water or soil. Among the different processes employed for water treatment, advanced oxidation processes (AOPs) are considered as promising technologies, involving the *in-situ* production of strong oxidants mainly hydroxyl radicals ($^{\bullet}OH$) at ambient pressure and temperature conditions (Andreozzi et al., 1999; Oturan and Aaron, 2014). This strong oxidant has a high standard reduction potential ($E° = 2.80$ V/SHE), reacting with organic compounds and giving unselective mineralization to CO_2, H_2O and inorganic ions.

Unfortunately, lindane oxidation entails serious difficulties due to the intrinsic characteristics of the molecule. It was already reported that lindane is less prone to oxidation than other organochloride compounds due to its non-aromatic and saturated structure and the absence of a double bond (Dionysiou et al., 2000). Moreover, the presence of electron-withdrawing chlorine groups in its molecular structure makes lindane even more resistant towards oxidation by $^{\bullet}OH$. In this sense and due to the difficulty of the challenge, various AOPs have been tested for lindane degradation: ozonation (Begum and Gautam, 2012), activated oxone (Wacławek et al., 2016), activated persulfate (Peng et al., 2015), the Fenton process (Usman et al., 2014), photolysis (Grannas et al., 2012) and mainly photocatalytic processes (Dionysiou et al., 2000; Fu et al., 2004; Senthilnathan and Philip, 2010) and combinations of different

oxidants with UV light (Nienow et al., 2008; Nitoi et al., 2013; Khan et al., 2017b). Surprisingly, electrochemical advanced processes (EAOPs) have been scarcely used for lindane removal from water. EAOPs are environmentally friendly emerging methods for the decontamination of wastewaters polluted with toxic and/or persistent pesticides, among other pollutants (Chaplin, 2014; Rodrigo et al., 2014; Martinez-Huitle et al., 2015) based on the direct production (anodic oxidation, AO) or indirect generation via Fenton's reagent (electro-Fenton, EF) of $^{\bullet}OH$. Recently the EF process has been successfully tested for the treatment of lindane polluted waters (Dominguez et al., 2017, 2018) with very interesting results. However, the electrooxidation (also called "anodic oxidation", AO) process, the most common electrochemical method for the treatment of organic pollutants due to its versatility and ease of scalability (Martínez-Huitle and Brillas, 2009; Vasudevan and Oturan, 2014, Garcia-Segura et al., 2018), has not yet been tested for the treatment of lindane wastewater.

AO is a clean process using only electrons as a reagent without the addition of chemicals to generate the oxidant species ($^{\bullet}OH$) in a wide range of pH conditions (Rodrigo et al., 2001; Panizza and Cerisola, 2009, de Araújo et al., 2014). In AO, organic pollutants are mainly degraded by adsorbed $^{\bullet}OH$ (Eq. 2) formed as intermediates from water oxidation at the surface of a high O_2-overvoltage anode (M) according to Eq. 1 (Panizza and Cerisola, 2009; Chaplin, 2014).

$$M + H_2O \rightarrow M(^{\bullet}OH) + H^+ + e^- \quad \text{(Eq. 1)}$$

$$\text{Organic pollutants} + M(^{\bullet}OH) \rightarrow M + CO_2 + H_2O + \text{inorganic ions} \quad \text{(Eq. 2)}$$

where $M(^{\bullet}OH)$ indicates the adsorbed hydroxyl radical at the anode surface (Eq. 2). The kinetics and efficiency of organic pollutant degradation in this process are mainly governed by the electrocatalytic properties of the anode material (Garcia-Segura et al.,

2018) and the applied current that governs the concentration and activity of heterogeneous •OH formed on its surface.

In this paper, the oxidative degradation of lindane and the mineralization of its aqueous solution was studied for the first time by the AO process using three of the most common anodes in EAOPs: Pt, DSA (dimensionally stable anode) and BDD (boron doped diamond) (Brillas et al., 2009; Sopaj et al., 2016). The role of the cathodic material such as carbon felt (CF), carbon sponge (CS) and stainless steel (SS) was also investigated. The influence of current density, the most determinant parameter in EAOPs, was optimized for efficient lindane degradation. Finally, based on the oxidation reaction intermediates identified during electrolysis, a plausible degradation pathway was proposed for lindane electrooxidation.

2. Materials and Methods

2.1. Reagents

Synthetic lindane solution was prepared by dissolving lindane (Fluka) in milli-Q water (10 mg L^{-1}) and shaking until the complete dissolution of the pollutant, which was checked by TOC (total organic carbon) measurements, corresponding to 2.45 mg L^{-1}. Working standard solutions of lindane, $C_8H_5KO_4$ (Nacalai Tesque), NaCl, $NaClO_3$ and $NaClO_4$ (Sigma-Aldrich) were prepared for gas chromatography - mass spectrometry (CG-MS), TOC and ionic chromatography (IC) calibration curves, respectively. Additional standard solutions of chlorinated compounds, hydroxylated compounds and carboxylic acids were also prepared in order to identify the reaction intermediates of lindane electrooxidation.

Other reagents (analytical grade) used in the present work were: C_3H_6O (acetone, Sigma Aldrich), Na_2SO_4 (Sigma-Aldrich), Na_2CO_3 (Riedel-de Häen), $NaHCO_3$ (Fluka),

CH_3OH and H_2SO_4 (Sigma-Aldrich). All the solutions were prepared with high-purity water obtained from a Millipore Direct-Q system with resistivity >18 MΩ cm at 25 ºC.

2.2. Electrochemical experiments

Although the concentration of lindane usually found in real effluents is significantly lower, experiments were carried out using lindane solutions at its solubility limit (10 mg L^{-1}) in order to facilitate its measurement, determination of TOC abatement, the release of chloride ions and the intermediate compounds generated during the electrochemical process.

Electrochemical experiments were performed over 6 hours in an undivided cylindrical glass cell with a volume capacity of 230 mL at room temperature (25 ± 1 ºC) and at the natural pH of lindane solution ($pH_0 \approx 6.5$). A 3D 90 cm^2 CF (18.0 cm × 5.0 cm × 0.5 cm, from Mersen, France) was used as the cathode in standard experiments. It was placed on the inner wall of the cell, covering the total internal perimeter. The anode commonly used was a 24 cm^2 BDD film on a niobium support (from CONDIAS GmbH, Germany), centered in the electrolytic cell. Preliminary experiments were performed in order to select the most suitable electrodes for lindane degradation and mineralization. Pt (24 cm^2, from Goodfellow, France) and DSA (Ti/RuO_2-IrO_2, 24 cm^2, from Baoji Xinyu GuangJiDian Limited Liability Company, China) were also tested as anode materials, while 21 cm^2 CS (6 cm x 3.5 cm x 1 cm, from Electrocell Europe (Denmark)) and SS (24 cm^2, from Goodfellow, France) were used as cathodes. According to the electrochemical cell configuration, the processes were denoted as BDD-CF (BDD anode, CF cathode), Pt-CF (Pt anode, CF cathode), DSA-CF (DSA anode, CF cathode), BDD-CS (BDD anode, CS cathode) and BDD-SS (BDD anode, SS cathode). Sodium sulfate (Na_2SO_4, 50 mM) was added to the cell as the background electrolyte in order to

144 increase solution conductivity. Lindane solution was continuously agitated by a
145 magnetic stirrer (250 rpm) to ensure an adequate mass transfer to/from electrodes and
146 the reactor was capped to avoid water evaporation and organics volatilization during the
147 electrolysis period. Once the electrode materials had been selected, a range of constant
148 currents from 100 to 800 mA (which correspond to current densities from 2.08 to 16.66
149 mA cm^{-2} taking into account the exposed anode surface, 48 cm^2) was applied to the
150 electrochemical cell. The current intensity and the potential difference of the cell were
151 measured and displayed continuously throughout electrolysis by using a DC power
152 supply (HAMEG Instruments, HM 8040-3). The change of solution pH during
153 electrolysis was monitored using a CyberScan pH1500 device from EUTECH
154 Instruments. All the experiments were performed in duplicate and the standard deviation
155 was lower than 5% in all cases.

156 *2.3. Analytical methods*

157 Lindane was identified and quantified by means of GC-MS analyses. Prior to analyses,
158 lindane and its oxidation intermediates in aqueous phase were extracted by using solid-
159 phase cartridges (C18-E, 55 μm, 70 Å, Phenomenex) and eluted with the same volume
160 of acetone (other solvents such as n-hexane, dichloromethane and ethyl acetate were
161 also tested). For the extraction process, an SPE Varian vacuum manifold-20 port model
162 and a KNF vacuum pump were used. Cartridges were preconditioned with acetone and
163 the aqueous matrix of the sample. Prior to acetone elution, cartridges were vacuum-
164 dried (10 mmHg) for 10 min to remove any trace of water. In order to minimize
165 experimental error in lindane quantification, 4-methylcyclohexanone was added to the
166 extracted samples as the internal standard compound (ISTD). Lindane calibration in the
167 range 0.025 - 10 mg L^{-1} was previously performed following the same extraction
168 procedure and compared with known concentrations of lindane directly dissolved in

169 acetone. The percentage of lindane recovery after the extraction process was covered
170 between 90 and 100%.

171 The Thermo Fisher Scientific (Trace 1300-ISQ) GC–MS used in this work was
172 equipped with a TG-5-MS column. Helium was used as the carrier gas with a flow rate
173 of 1.2 mL min^{-1}. The GC injection port temperature was set at 250 °C. Extracted
174 samples (3 µL) were manually injected. The program temperature started at 40 °C (held
175 for 2 min) followed by a temperature ramp of 10 °C min^{-1} to 280 °C and then held
176 constant for 4 min. Analysis was carried out in EI mode (70 eV).

177 The decay in TOC solution was measured by a Shimadzu TOC-V_{CSH} analyzer.
178 Reproducible TOC values with an accuracy of ± 2% were determined using the non-
179 purgeable organic carbon method. Calibration was achieved with potassium hydrogen
180 phthalate solutions.

181 Aromatic intermediates were identified by HPLC, using a Merck HITACHI LaChrom
182 liquid chromatograph equipped with an L-2310 pump, fitted with a reverse phase
183 Purospher RP-18, 5 µm, 25 cm × 4.6 mm (i.d.) column and coupled with an L-2400 UV
184 detector set at λ = 238 nm. The temperature of the column was maintained constant at
185 40 °C, the injection volume was 20 µL and the isocratic eluent 30:70 methanol/water
186 was pumped to the system at a flow rate of 0.5 mL min^{-1}.

187 Generated carboxylic acids were identified by ion-exclusion HPLC using a Merck
188 HITACHI LaChrom Liquid chromatography system equipped with an L-7100 pump
189 fitted with a Supelcogel H (9 µm, 25 cm × 4.6 mm) column at room temperature and
190 coupled with a DAD-UV L-7455 detector set at λ = 220 nm, using 1% H_2SO_4 at 0.2 mL
191 min^{-1} as the mobile phase.

192 The dechlorination degree was evaluated in terms of chloride ions released to the
193 solution during electrolysis, which were determined by IC (930 Compact IC Flex,
194 Metrohm) with anionic chemical suppression equipped with a conductivity detector and
195 an autosampler (910 IC autosampler plus). An anionic exchanger column (Metrosep A
196 Supp5-250/4, 25 cm length, 4 mm diameter) was used as the stationary phase and 0.7
197 mL min^{-1} of an aqueous solution 3.2 mM of Na_2CO_3 and 1 mM of $NaHCO_3$ as the
198 mobile phase. Other chlorine species, such as chlorate and perchlorate ions during
199 electrolysis were also followed by this technique.
200

201 **3. Results and discussion**

202 3.1. Effect of electrode materials on lindane degradation

203 The choice of electrode material determines the efficiency of electrooxidation process
204 as well as the potential formation of toxic by-products (Radjenovic and Sedlak, 2015).

205 *3.1.1 Anode materials*

206 The time-course of lindane concentration and solution TOC with different anode
207 materials tested under selected operating conditions is shown in Figs. 1a and 1b,
208 respectively. In these experiments, the same cathode (CF) was used for the sake of
209 comparison. A control experiment without current intensity was also performed,
210 obtaining negligible changes both in pollutant concentration and TOC value at 6 h (data
211 not shown), keeping the solution volume constant (which was also checked during
212 electrochemical experiments). Therefore, water evaporation and/or lindane adsorption
213 on the electrodes during the treatment time were insignificant.

214 It was observed that lindane degradation was relatively fast; in the worst case, 30 min
215 was enough to completely degrade the pollutant with a current density of 8.33 mA cm^{-2}.

However, different oxidation rates were obtained depending on the anode used, BDD being the most efficient anode.

During the electrooxidation process, organic compounds are mainly oxidized by indirect oxidation via oxidants generated on the anode surface such as heterogeneous $^{\bullet}OH$ (M($^{\bullet}OH$)), the second most powerful oxidant after fluorine (Panizza and Cerisola, 2009). As shown in Fig. 1, oxidative degradation of lindane and mineralization of its solution was quicker with a BDD anode than with Pt and DSA anodes. This more efficient oxidation power of the BDD anode could be related to its greater O_2-evolution overvoltage compared to the active anodes, Pt and DSA (Panizza and Cerisola, 2005; Brillas et al., 2009; Barhoumi et al., 2015). Thus, the BDD anode produced a higher amount of reactive BDD($^{\bullet}OH$) from the electrochemical oxidation of water (Eq. 1) and minimized the production of competitive reactions (Eq. 3) that consume the radical species leading to oxygen production (Garcia-Segura et al., 2018).

$$2\ M(^{\bullet}OH) \rightarrow 2\ M + O_2 + 2\ H^+ + 2\ e^- \qquad \text{(Eq. 3)}$$

Additionally, the BDD($^{\bullet}OH$) is weakly adsorbed (physisorption) on the anode surface, thus being easily available for oxidation of organics present in the vicinity of the anode. In contrast, Pt and DSA anodes present relatively weak O_2-evolution overpotential with chemisorbed M($^{\bullet}OH$), which is less mobile to efficiently oxidize organic pollutants (Oturan et al., 2013). Moreover, the active anodes are capable of oxidizing organics into more biodegradable molecules but they cannot achieve their complete transformation into carbon dioxide (Garcia-Segura et al., 2018).

The DSA anode led to a slightly higher lindane oxidation rate than the Pt anode (Fig. 1a), probably due to the formation of hypochlorite on the anode surface from the

oxidation of chloride ions, these coming from lindane degradation according to its mineralization reaction (Eq. 4):

$$C_6H_6Cl_6 + 12\ H_2O \rightarrow 6\ CO_2 + 6\ Cl^- + 30\ H^+ + 24\ e^- \quad \text{(Eq. 4)}$$

The oxidation of chloride anions on the anode surface by direct electrooxidation and/or by the indirect action of reactive oxygen species, M(•OH) (the DSA and to a greater extent, the BDD anodes), leads to the formation of active chlorine species (Eqs. 5 to 7), which are powerful oxidants that can play an important role in the oxidation of organics via "mediated oxidation" (Deng and Englehardt, 2007; Canizares et al., 2009; Panizza and Cerisola, 2009, Randazzo et al., 2011; Brillas and Martínez-Huitle, 2015). These chlorine species are the main indirect oxidation agents employed in wastewater treatment (Moreira et al., 2017).

Firstly chloride is oxidized on the anode surface releasing chlorine (Eq. 5). When the electrogenerated chlorine diffuses away from the anode, it is quickly hydrolyzed yielding hypochlorous acid (HClO) and chloride by disproportionation (Eq. 6). HClO is in equilibrium with the hypochlorite ion (ClO^-) with pKa=7.55 (eq. 7). The predominance of these species is a function of solution pH: ClO^- (pH above 7), HClO (from pH 7 to 3) and Cl_2 (pH below 3), respectively (Moreira et al., 2017). It should be noted that the starting pH of the lindane solution (6.5) rapidly decreased in all cases to values of about pH 3 - 3.5 after 30 min of electrolysis (see sub-section 3.2). Thus, hypochlorous acid predominates during the whole process. Otherwise, the standard reduction potential of Cl_2 (aq) (E° = 1.36 V/SHE) and HClO (E° = 1.49 V/SHE) is considerably higher than ClO^- (E° = 0.89 V/SHE), indicating that oxidation of organics, mediated by chlorine active species, is favored under acidic pH conditions (Moreira et al., 2017, Garcia-Segura et al., 2018).

263 $2\ Cl^- \rightarrow Cl_2\ (aq) + 2\ e^-$ (Eq. 5)

264 $Cl_2\ (aq) + H_2O \rightarrow HClO + Cl^- + H^+$ (Eq. 6)

265 $HClO \leftrightarrow H^+ + ClO^-$ (Eq. 7)

266 Less active chlorine species (chlorite, chlorate and perchlorate anions, $E^\circ < 1$ V/SHE in
267 all cases) can be simultaneously generated by the action of M($^\bullet$OH) according to the
268 following equations (Eqs. 8-11, Hubler et al., 2014). This phenomenon is especially
269 important in the case of non-active anodes (Garcia-Segura et al., 2018), such as BDD.
270 When using BDD anodes, chloride completely transformed to form perchlorate in long-
271 term discontinuous experiments and/or if large current charges were passed through the
272 cell (Bergmann et al., 2009, 2011).

273 $Cl^- + M(^\bullet OH) \rightarrow ClO^- + 2\ H^+$ (Eq. 8)

274 $ClO^- + M(^\bullet OH) \rightarrow ClO_2^- + 2\ H^+$ (Eq. 9)

275 $ClO_2^- + M(^\bullet OH) \rightarrow ClO_3^- + 2\ H^+$ (Eq. 10)

276 $ClO_3^- + M(^\bullet OH) \rightarrow ClO_4^- + 2\ H^+$ (Eq. 11)

277 The latter generated chlorine species (ClO_3^- and ClO_4^-) are unwanted by-products since
278 they are hydroxyl radical-consuming and are not able to oxidize organics in solution
279 (Garcia-Segura et al., 2015). Moreover, these species, considered noxious (especially
280 perchlorate), are of great concern as inorganic pollutants in water sources (van Wijk et
281 al., 1998, Ting and Steinmaus, 2013, Garcia-Segura et al., 2018). Water effluents
282 containing greater amounts of chloride ions favor the generation of high concentrations
283 of these species, limiting their electrochemical treatment. The amount of chlorinated
284 organic by-products may be minimized by applying a short electrolysis time while

targeting a suitable degree of removal of contaminants. If these compounds (chlorate, perchlorate) are formed in concentrations higher than those allowed, they could be removed by adsorption on activated carbon, ion-exchange, membrane filtration, and microbial, chemical or electrochemical reduction (Radjenovic and Sedlak, 2015). On the other hand, it should be noted that ClO_4^- poses no problem when it is generated in low or moderate concentrations (the maximum concentration of chlorine in this study was that from the lindane molecule, 7.43 mg L^{-1}). Moreover, its salts are even used as an electrolyte in EAOPs (Diagne et al., 2007, Hubler et al., 2014, Radjenovic and Sedlak, 2015). On the other hand, a study concerning the toxicity of chlorate on selected species of algae, bacteria, and fungi confirmed that chlorate is toxic only to brown algae and not to species of other ecologically important taxa (van Wijk et al., 1998).

The change of Cl^- and ClO_3^- ion concentrations (the most important chlorine species identified in terms of concentration) during lindane electrooxidation with the different electrodes tested was monitored by IC and results are shown in Fig. 2. With regard to the other chlorine species, ClO^- could not be measured; ClO_2^- appeared only in trace amounts (below the detection limit) and ClO_4^- was only detected when the BDD anode was used (Radjenovic and Sedlak, 2015). A possible explanation to justify the detection of ClO_2^- in such low concentrations is the direct electrochemical conversion of hypochlorous acid to chlorate ion according to Eq. 12 (Moreira et al., 2017):

$$6\ HClO + 3\ H_2O \rightarrow 2\ ClO_3^- + 4\ Cl^- + 12\ H^+ + 1.5\ O_2 + 6\ e^- \qquad \text{(Eq. 12)}$$

Pt, despite being an active anode, seems to be the only one unable to oxidize chlorides (Eqs. 5 and 8). The concentration of Cl^- in the Pt/CF cell increased until reaching a maximum value of around 7 mg L^{-1} after 2 h electrolysis time. From this point, the concentration of chlorides in the reaction medium remained constant. This value represents almost 95% of the theoretical amount of chlorine initially present in lindane

(7.43 mg L^{-1}) according to Eq. 4, suggesting its complete dechlorination. The slight mismatch (5%) may be due to the analytical errors or presence of some organochlorines that remain in the solution since the mineralization achieved was not total. Regarding the DSA anode, the formation of Cl^- followed the same trend as with the Pt anode until 2 h electrolysis. From this time, the chloride concentration slightly decreased as a consequence of its oxidation to active chlorine species on the anode surface. This fact was corroborated by the formation of ClO_3^- almost from the beginning of the reaction, which implies the previous generation of ClO^- and ClO_2^- and, therefore, the oxidation of Cl^-.

The release of chloride was faster in the BDD-CF cell as a result of the faster lindane oxidation in the presence of the BDD anode (Fig. 1a). The maximum value of Cl^- (5 mg L^{-1}) was reached at 30 min electrolysis. Once generated, chlorides are rapidly oxidized into the other chlorine species by the indirect action of M(•OH) (Eqs. 8-11). In this case, the chlorate anion (and hence ClO^- and ClO_2^-) appeared practically from the beginning of the reaction. This anion achieved its maximum concentration value at 2 h of electrolysis. Afterwards, its concentration decreased progressively, giving rise to the formation of ClO_4^-. Perchlorate was detected from 60 min of electrolysis (0.87 mg L^{-1}) and its concentration was always increasing until reaching 3.83 mg L^{-1} at the end of the treatment.

The effect of oxidation mediated by active chlorine species (ClO^-, HClO and Cl_2) did not bring a positive effect on the mineralization efficiency when using the DSA anode. In this case, TOC removal was lower than that obtained with the Pt-CF system. The influence of chloride concentration on the electrooxidation of leachates has been studied, concluding that indirect oxidation using chloride/hypochlorite requires a high chloride concentration, typically larger than 3000 mg L^{-1} (Deng and Englehardt, 2007;

Chen, 2004). Therefore, although the active chlorine species formed in the presence of DSA (ClO^-, HClO and Cl_2) showed little effect on lindane oxidation rate (first min of reaction), they were not strong enough to oxidize lindane intermediates and carboxylic acids, possibly formed in the subsequent steps of the treatment (the oxidation power of all these species is significantly lower than that of M(•OH), from their standard reduction potentials). Moreover, the oxidation of chloride by M(•OH) to give the oxygenated chlorine-anions (ClO^-, ClO_2^-, ClO_3^- and ClO_4^-) negatively affects the mineralization efficiency of the process, consuming current density unproductively. This fact is also applicable to the BDD-CF system.

For large industrial applications, the treatment cost of the process is a very important parameter (Labiadh et al., 2015). In order to evaluate the economic factors, the specific energy consumption per unit TOC mass removed (EC_{TOC}) in kWh $(gTOC)^{-1}$ for each trial was determined by means of the following expression (Brillas et al., 2009):

$$EC_{TOC} = \frac{E_{cell}\, I\, t}{V\, \Delta TOC} \qquad \text{(Eq. 13)}$$

where E_{cell} is the average cell voltage (V), I is the applied current (A), t is the electrolysis time (h), V is the solution volume (L) and ΔTOC is the experimental TOC decay (mg L^{-1}) reached at time t. As can be seen in Fig. 3, in general, EC_{TOC} increased with the TOC removal degree as a consequence of the generation of less oxidizable compounds such as carboxylic acids with the progression of the mineralization process (Panizza and Cerisola, 2009; Sirés and Brillas, 2012; Sirés et al., 2014). The results of this figure indicate that the mineralization of lindane solution during electrooxidation using the Pt and DSA anodes consumed two and four times more energy, respectively, than the BDD anode. Moreover, these anodes also gave lower TOC removal performance under the same operating conditions (60% and 40% respectively *vs.* 80%

for BDD at 6 h). In summary, the BDD anode exhibited the best performance, both in oxidation power and mineralization degree, and energy consumption. Therefore, it was selected as the most suitable anode for following studies.

3.1.2 Influence of the cathode materials on electrooxidation of lindane

The role of the different cathodes is shown in Figs. 1c and 1d, all of them with the BDD anode. No differences were found either in lindane degradation or mineralization when CF and CS cathodes were used. However, the SS cathode led to lower lindane oxidation and mineralization degrees. This fact could be related to the generation of hydrogen peroxide on the cathode surface from the two-electron reduction of oxygen when CF and CS are used (Eq. 14). The efficiency of H_2O_2 electrogeneration depends on the contact between cathode, oxygen and water. For this reason, three-dimensional electrodes of high specific surface area such as porous carbonaceous materials are preferred. This process is also named AO-H_2O_2, anodic oxidation with electrogenerated H_2O_2 (Moreira et al., 2017).

$$O_2 + 2\,H^+ + 2\,e^- \rightarrow H_2O_2 \qquad \text{(Eq. 14)}$$

An additional experiment was carried out by adding an excess of H_2O_2 (100 mg L^{-1}) to a lindane solution (10 mg L^{-1}) (without current density) and negligible pollutant and TOC conversion during 6 h electrolysis time were obtained (Fig. 1 Supplementary Material). Therefore, it can be deduced that H_2O_2 by itself was not active enough at 25 ºC to oxidize lindane. H_2O_2 itself (E° = 1.77 V/SHE) is able to attack reduced sulfur compounds, cyanides and some organics such as aldehydes, formic acid and some nitroorganic and sulfoorganic compounds (Moreira et al., 2017). However, H_2O_2 generated on the cathode surface can be oxidized on the anode surface giving rise the formation of hydroperoxyl radicals $^{\bullet}OOH$ (Eq. 15, Oturan et al., 2013, Moreira et al.,

2017), (E° = 1.70 V/SHE) which can also contribute to the oxidation of lindane and its primary intermediates.

$$H_2O_2 \rightarrow H^+ + {}^{\bullet}OOH + e^- \quad \text{(Eq. 15)}$$

Regarding the active chlorine species formed with different cathodes, small differences were obtained, as can be seen in Fig. 2c. In all cases, a maximum value of Cl^- was obtained at 60 min electrolysis time, indicating that this species is further oxidized on the anode by direct electron transfer or by M($^{\bullet}OH$). The higher concentration of ClO_3^- determined in the presence of CS can be related to its very low oxidation to the ClO_4^- ion. Thus, the higher oxidation rate of ClO_3^- to ClO_4^- in the case of CF and CS cathodes could be explained by the probable contribution of H_2O_2 formed in the presence of these cathodes.

Regarding the energy consumption per unit TOC mass removed, the SS cathode exhibited high EC_{TOC} values compared with the CF and CS cathodes. These results could be explained by the longer electrolysis time required for the removal of an equivalent TOC value and also by the higher cell voltage developed in this case. Cells with CF and CS led to almost identical results in terms of EC_{TOC} values. However, it is worth noting that CF is more stable, mechanically more resistant and easier to handle. Thus, this cathode was selected as the most suitable for further lindane oxidation/mineralization experiments.

3.2. Change of solution pH

The change of pH was monitored over the course of electrooxidation of lindane for all the trials above cited. The results showed that pH decreased during electrolysis, especially more quickly during the first 30 min, until reaching a value of between 3 and 3.5 at the end of the experiments (Fig. SM 2). The pH drop is due to i) the release of H^+

to the reaction medium during the mineralization process according to Eq. 4 (Nienow et al., 2008), ii) the formation of short-chain carboxylic acids that provide a pH value close to 3 to the solution (these acids constitute the residual TOC remaining at the end of treatment) and iii) the progressive oxidation of chloride ions according to the reactions 9-12, generating H^+.

Once BDD and CF were selected as the most suitable electrodes, the influence of the initial pH was evaluated. For this purpose, an experiment at initial pH = 3 (H_2SO_4 1 M) was performed at 400 mA with the BDD-CF cell and the results were compared with those of the experiment carried out at a natural solution pH of 6.5; the other operating conditions were maintained constant. The results are shown in Fig. SM 3 and demonstrated very slight differences in lindane electrooxidation and mineralization. Therefore, natural pH was selected for further experiments.

3.3. Effect of current density on electrooxidation of lindane

The applied current, and therefore, current density, is the main key factor governing the effectiveness of the electrooxidation processes because it regulates the amount of M(•OH) that oxidizes organic matter present in the solution up to mineralization (Brillas et al., 2009; Sirés et al., 2014). To check the influence of this parameter on lindane oxidation and mineralization, current densities ranging from 2.08 to 16.67 mA cm^{-2} were applied to the BDD/CF cell, maintaining the other parameters constant. The potential difference of the cell increased with the current density (Fig. SM 4) and remained constant during electrolysis, indicating the absence of formation of non-conductive layers on the surface of the electrodes and corrosion of the electrodes materials during electrooxidation experiments (Canizares et al., 2007, 2009).

433 *3.3.1. Oxidative degradation of lindane*

434 Lindane concentration underwent a gradual decay during electrolysis as a function of
435 current density. As it can be seen in Fig. 4a, an increase in current density led to an
436 increase in lindane oxidation rate due to the higher production of M(•OH). Thereafter,
437 lindane conversions of 35%, 52%, 70% and 80% at 2.08, 4.17, 8.33 and 16.67 mA cm^{-2},
438 respectively, were achieved at 6 min of electrolysis. Lindane electrooxidation follows a
439 *pseudo*-first order reaction, which is fairly common in other AOPs for lindane
440 degradation such as photocatalysis (Khaydarov et al., 2013), the Fenton process (Begum
441 et al., 2014), the photo-Fenton process (Nitoi et al., 2013), ozonation (Begum and
442 Gautam, 2012) and activated persulfate (Khan et al., 2016).

443 The corresponding kinetic data are plotted in Fig. 4b and the relationship between the
444 apparent rate constant (k_{app}), calculated from the slope of the resulting straight lines
445 (following *pseudo*-first order kinetic analysis), and the current density is represented in
446 the inset of Fig. 4b. k_{app} values increased almost linearly with current density up to 8.33
447 mA cm^{-2}. Above this value, there were no significant improvements while higher
448 energy consumptions were required. Therefore, regarding lindane degradation, a current
449 density of 8.33 mA cm^{-2} can be considered the optimum value for lindane degradation
450 in the BDD/CF cell.

451

452 *3.3.2. Mineralization of lindane solution*

453 Change of solution TOC during electrooxidation at different current densities is
454 depicted in Fig. 5. As expected, the higher the current density, the higher the
455 mineralization rate. When working at 16.67 mA cm^{-2}, a TOC conversion of 70% was
456 achieved at 2 h electrolysis time, while at 2.08 mA cm^{-2}, only 40% of TOC depletion

was obtained. The mineralization current efficiency (MCE) was calculated for each experiment following Eq. 16 (Brillas et al., 2009; Borràs et al., 2010):

$$MCE\ (\%) = \frac{n\ F\ V\ \Delta TOC}{4.32\times10^{7}\ m\ I\ t} \times 100 \qquad \text{(Eq. 16)}$$

where *n* is the number of electrons consumed per lindane molecule (24) considering its complete mineralization (Eq. 4), *F* is the Faraday constant (96487 C mol^{-1}), *m* is the number of carbon atoms of lindane (6), and 4.32×10^{7} is the conversion factor to homogenize the units (3600 s h^{-1}·12000 mg C mol^{-1}).

Figs. 6a and 6b collect the effect of current density on MCE and EC per percentage of TOC removed. MCE decreased progressively with electrolysis time as result of the generation of more recalcitrant compounds, such as carboxylic acids and the consequent loss of organic matter (Brillas et al., 2009; Sirés et al., 2014). On the other hand, this parameter increased as the current density decreased. Thus, MCE was 5 times higher at 2.08 mA cm^{-2} than at 16.67 mA cm^{-2}. This decay is typical in EAOPs (Barhoumi et al., 2015) and can be explained by the increase of rate of parasitic reactions due to the excess of hydroxyl radicals such as dimerization of M(•OH) and the loss of energy consumed in side reactions such as H_2 production on the cathode. It should be noted that MCE values in all cases were quite low (<1.2%) as a consequence of the low initial TOC concentration (2.45 mg L^{-1}).

Regarding the change of EC_{TOC}, it slightly increased with low TOC removal values while becoming exponential for higher TOC removals (>70%), making the process much more expensive, mainly at 16.67 mA cm^{-2}. This behavior can be also explained by i) the formation of more refractory products, such as short-chain carboxylic acids, which are difficult to oxidize intermediates, and by ii) a decrease in the organic carbon content of the solution, which promotes the enhancement of parasitic reactions (Barhoumi et al.,

2015; Labiadh et al., 2015). The lowest energy consumption was achieved at 2.08 mA cm^{-2}, as expected by the lower cell potential (Fig. SM 4); this current density leading also to the highest MCE value (Fig. 6a). In contrast, the energy consumption increased significantly reaching much higher values for the experiment carried out at 16.67 mA cm^{-2}. In this trial, the EC_{TOC} for 80% TOC removal reached 60 kWh $(g\ TOC)^{-1}$, being more than two times higher (25 kWh $(gTOC)^{-1}$) than that consumed at 8.33 mA cm^{-2} for the same TOC removal rate. According to these results, 8.33 mA cm^{-2} was the best current density value that could be used in the electrooxidation of lindane for an effective mineralization.

Finally, no differences in terms of pH were found at the end of the experiments, these values being between 3.1 and 3.45 for the different current densities tested.

3.3.3. Dechlorination of lindane during electrooxidation

Chloride appeared from the beginning of the treatment. The release of this anion to the solution was proportional to the extent of the lindane oxidation process. Therefore, the concentration of Cl^- in the reaction media increased with current density in the early stages of reaction and reached the maximum value at about 15 min for the high current density values of 8.33 and 16.67 mA cm^{-2} (Fig. 7a). On the other hand, once generated, Cl^- was oxidized at the BDD anode surface by direct electron transfer or by BDD(•OH) to Cl_2 and further to other active chlorine species (Eqs. 5 to 7). Therefore its concentration decreased after 15 min electrolysis. This decrease was greater at higher current densities; for instance, the maximum concentration of Cl^- (3.7 mg L^{-1}) attained after 15 min of electrolysis, decreased until reaching 0.4 and 0.2 mg L^{-1} for 8.33 and 16.67 mA cm^{-2}, respectively, at the end of treatment. The concentration of ClO_3^- (Eqs. 10 and 12), the second most abundant chlorine species (Fig. 7b), increased with

electrolysis time and current density to reach a maximum at 2 and 1 h of electrolysis in the experiments carried out at 8.33 and 16.67 mA cm^{-2}, respectively, while ClO_2^- appeared only in trace amounts. From this moment, ClO_3^- decreased as a consequence of its oxidation to ClO_4^-, the concentration of which increased to the end of the experiment. When working with current densities of 2.08 and 4.17 mA cm^{-2}, the change of ClO_3^- with electrolysis time always increased since these current density values were not enough for its oxidation to ClO_4^-.

Summing up the measured chlorine ions (Cl^-, ClO_3^- and ClO_4^-), it is possible to quantify up to 80% of total chlorine from lindane. The remaining percentage is attributed to the formation of other unmeasured chlorinated ions such as ClO^-, and, to a lesser extent, to the formation of chlorinated carboxylic acids, such as chloroacetic acid at a concentration below the detection limit.

3.4. Product identification and oxidation pathway

As previously commented, lindane oxidation was much faster than its mineralization (see Figs. 4 and 5), indicating the formation of intermediate products prior to its conversion to CO_2. Moreover, there was also a delay between lindane oxidation and the release of chlorides to the reaction medium (see Figs. 4 and 7), which suggests the formation of chlorinated intermediates in the early stages of the process.

To understand the reaction mechanism of lindane electrooxidation and establish the oxidation reaction pathway, an attempt to identify the different oxidation intermediates was made. In order to facilitate intermediate identification, electrolysis experiments were carried out at the lowest current density of 2.08 mA cm^{-2}. At this current density, the lindane oxidation rate is slow and the accumulation of intermediates is favored because of their low degradation rates. Identification of intermediates was performed by

GC-MS (after liquid-solid phase extraction), reversed-phase HPLC and ion-exclusion HPLC analyses. The identification of lindane intermediates by GC-MS was assessed with the aid of the NIST database library and by HPLC from comparison of their retention times and UV-VIS spectrum with those of standard compounds.

Seven chlorobenzenes (chlorobenzene, 1,2 and 1,4 dichlorobenzene, 1,3,5 and 1,2,4 trichlorobenzene, 1,2,3,5 and 1,2,4,5 tetrachlorobenzene), two chlorocyclohexenes (tetrachlorocyclohexene and pentachlorocyclohexene), two chlorophenols (2,4 dichlorophenol, 1,2,4 trichlorophenol) and hydroxyquinol were identified in trace amounts from the beginning of the reaction (from 5 to 60 min, at 100 mA). The formation of a great variety of intermediates prior to mineralization suggests a complex mechanism of degradation, in which, several processes, i.e., chlorination, dechlorination, hydrogenation, dehydrogenation, hydroxylation, etc., take place at about the same time in parallel and serial reactions.

In the first place, chlorine and hydrogen atoms are abstracted from the Cl-C-H groups (constituting the lindane molecule) forming penta- and tetrachlorocyclohexene (Wacławek et al., 2016), the predominant intermediate compounds (in terms of peak area). Chlorobenzenes could be formed through progressive reductive dechlorination of these by-products resulting in less substituted chlorobenzenes (Zinovyev et al, 2004). Simultaneously, these compounds could be attacked by·˙OH leading to the formation of hydroxylated compounds such as 2,4 dichlorophenol, 1,2,4 trichlorophenol and hydroxyquinol. All these compounds are more susceptible to attack by ˙OH than lindane (Oturan and Aaron, 2014), as the addition of ˙OH is more favored on the aromatic ring than the abstraction of the hydrogen atom from lindane (non-aromatic structure and the absence of a double bond). Accordingly, these cyclic compounds disappeared from relatively short electrolysis times (between 15 and 60 min), after which time some

carboxylic acids (succinic, oxalic, acetic and formic acids) were detected as a result of ring cleavage reactions. Carboxylic acids are finally transformed into CO_2 and water (Brillas et al., 2009). Among low-molecular-weight organic compounds, formic acid was the most abundant, with a maximum concentration of 1.1 mg L^{-1} at 60 min, decreasing subsequently to 0.15 mg L^{-1} at the end of the electrochemical treatment. It was the only organic compound identified at the final electrolysis time of 6 h. It has to be noted that chlorine atoms were released in subsequent stages as chloride ions.

On the basis of the above results, a simplified and plausible reaction pathway for lindane electrooxidation with the BDD/CF system has been established (Fig. 8). The identified compounds have been grouped attending to their nature into "cyclic chlorinated by-products", "cyclic hydroxylated by-products" and "carboxylic acids". The main reactions involved in lindane electrooxidation are dechlorination and hydroxylation of the pollutant (and its by-products) followed by C–C bond cleavage. The attack by BDD($^{\bullet}$OH) on the chlorine positions of lindane results in replacement of these atoms with hydroxyl groups on the six-carbon ring. Further attack leads to the rupture of the C–C bonds and therefore ring-opening, followed by oxidation to short-chain carboxylic acids (Oturan et al., 2008; Almeida et al., 2011; El-Ghenymy et al., 2014). Data obtained from different analyses are consistent with the final products of the proposed pathway.

4. Conclusions

This study reports for the first time the effective degradation of lindane by an electrochemical advanced oxidation process, which was shown to be a highly efficient technology for the oxidation of lindane and the mineralization of its aqueous solution. The best results, taking into account lindane oxidation, mineralization of its aqueous

581 solution and cost-effectiveness, were obtained by using the BDD anode compared to the
582 other anodes tested, *i.e.*, Pt and DSA. Regarding the cathodic material, CF was the most
583 convenient cathode due to the lowest specific energy consumption per unit TOC mass
584 removed in addition to its high stability and greater ease of handling compared to the SS
585 and CS cathode materials. A current density of 8.33 mA cm^{-2} was found to be the best
586 value for complete lindane oxidation at about 10 min, resulting in a high mineralization
587 degree (>80% at 4 h) and a relatively low energy consumption (15 kWh $(gTOC)^{-1}$)).
588 The oxidative lindane degradation by *in-situ* generated hydroxyl radicals followed
589 *pseudo* first-order reaction kinetics. A plausible reaction pathway for lindane oxidation
590 by M(•OH) has been proposed based on the identified chlorinated and hydroxylated
591 intermediates and the resulting short-chain carboxylic acids. Chlorine atoms were
592 mineralized to chloride ions in a first stage and then progressively oxidized to active
593 chlorine species during the electrolysis.

594

595 **Acknowledgments**

596 The authors acknowledge financial support from the Comunidad Autónoma of Madrid
597 (Project S2013-MAE-2739 CARESOIL-CM) and from the Spanish Ministry of
598 Economy and Competitiveness (Project CTM2013-43794-R) and the Université Paris-
599 Est Marne-la-Vallée (France) for research facilities. Carmen M. Domínguez
600 acknowledges the Spanish MICINN for the "Juan de la Cierva" post-doctoral grant and
601 the "José Castillejo" mobility program.

602

603

604 **REFERENCES**

605 Almeida, L. C., Garcia-Segura, S., Bocchi, N., Brillas, E., 2011. Solar photoelectro-
606 Fenton degradation of paracetamol using a flow plant with a Pt/air-diffusion cell
607 coupled with a compound parabolic collector: process optimization by response
608 surface methodology. Appl. Catal. B: Environ., 103 (1), 21-30.

609 Andreozzi, R., Caprio, V., Insola, A., Marotta, R., 1999. Advanced oxidation processes
610 (AOP) for water purification and recovery. Catal. Today 53 (1), 51-59.

611 Barhoumi, N., Labiadh, L., Oturan, M. A., Oturan, N., Gadri, A., Ammar, S., Brillas, E.,
612 2015. Electrochemical mineralization of the antibiotic levofloxacin by electro-
613 Fenton-pyrite process. Chemosphere, 141, 250-257.

614 Begum, A. and Gautam, S. K., 2012. Endosulfan and lindane degradation using
615 ozonation. Environl technol., 33 (8), 943-949.

616 Begum, A., Agnihotri, P., Mahindrakar, A. B., Gautam, S. K., 2014. Degradation of
617 endosulfan and lindane using Fenton's reagent. Appl. Water Sci. 7, 1-9.

618 Behrooz, R. D., Sari, A. E., Bahramifar, N., Ghasempouri, S., 2009. Organochlorine
619 pesticide and polychlorinated biphenyl residues in human milk from the Southern
620 Coast of Caspian Sea, Iran. Chemosphere, 74 (7), 931-937.

621 Bergmann, M. E. H., Iourtchouk, T., Schmidt, W. Nüske, G., Fischer, M., 2011.
622 Perchlorate formation in electrochemical water disinfection. Paperback Imprint
623 Nova Science, New York, ISBN: 13: 9781612096902.

624 Bergmann, M. H., Rollin, J., Iourtchouk, T., 2009. The occurrence of perchlorate during
625 drinking water electrolysis using BDD anodes. Electrochim. Acta, 54 (7), 2102-
626 2107.

627 Borràs, N., Oliver, R., Arias, C., Brillas, E., 2010. Degradation of atrazine by
628 electrochemical advanced oxidation processes using a boron-doped diamond anode.
629 J. Phys. Chem. A, 114 (24), 6613-6621.

630 Brillas, E. and Martínez-Huitle, C. A., 2015. Decontamination of wastewaters
631 containing synthetic organic dyes by electrochemical methods. An updated review.
632 Appl. Catal. B: Environ., 166-167, 603-643.

633 Brillas, E., Sirés, I., Oturan, M. A., 2009. Electro-Fenton process and related
634 electrochemical technologies based on Fenton's reaction chemistry. Chem. Rev.,
635 109 (12), 6570-6631.

636 Camacho-Pérez, B., Ríos-Leal, E., Rinderknecht-Seijas, N., Poggi-Varaldo, H. M.,
637 2012. Enzymes involved in the biodegradation of hexachlorocyclohexane: a mini
638 review. J. Environ. Manage., 95, S306-S318.

639 Canizares, P., Hernández-Ortega, M., Rodrigo, M., Barrera-Díaz, C., Roa-Morales, G.,
640 Sáez, C., 2009. A comparison between conductive-diamond electrochemical
641 oxidation and other advanced oxidation processes for the treatment of synthetic
642 melanoidins. J. Hazard. Mater., 164 (1), 120-125.

643 Canizares, P., Lobato, J., Paz, R., Rodrigo, M., Sáez, C., 2007. Advanced oxidation
644 processes for the treatment of olive-oil mills wastewater. Chemosphere, 67 (4),
645 832-838.

646 Chang, C., Lian, F., Zhu, L., 2011. Simultaneous adsorption and degradation of gamma-
647 HCH by nZVI/Cu bimetallic nanoparticles with activated carbon support. Environ.
648 Pollut., 159 (10), 2507-2514.

649 Chaplin, B.P., 2014. Critical review of electrochemical advanced oxidation processes
650 for water treatment applications. Environ. Sci. Proc. Imp. 16, 1182–1203.

651 Chen, G., 2004. Electrochemical technologies in wastewater treatment. Separ. Purif.
652 Technol., 38 (1), 11-41.

653 de Araújo, D. M., Cañizares, P., Martínez-Huitle, C. A., Rodrigo, M. A., 2014.
654 Electrochemical conversion/combustion of a model organic pollutant on BDD
655 anode: Role of sp3/sp2 ratio. Electrochem. Commun. 47, 37–40.

656 Deng, Y. and Englehardt, J. D., 2007. Electrochemical oxidation for landfill leachate
657 treatment. Waste Manage., 27 (3), 380-388.

658 Diagne, M., Oturan, N., Oturan, M. A., 2007. Removal of methyl parathion from water
659 by electrochemically generated Fenton's reagent. Chemosphere, 66 (5), 841-848.

660 Dionysiou, D. D., Khodadoust, A. P., Kern, A. M., Suidan, M. T., Baudin, I., Laîné, J.,
661 2000. Continuous-mode photocatalytic degradation of chlorinated phenols and
662 pesticides in water using a bench-scale TiO2 rotating disk reactor. Appl. Catal. B:
663 Environ. 24 (3), 139-155.

664 Dominguez, C. M., Oturan, N., Romero, A., Santos, A., Oturan, M. A., 2017.
665 Optimization of electro-Fenton process for effective degradation of organochlorine
666 pesticide lindane. Catal. Today. *In press.*

667 Dominguez, C. M., Oturan, N., Romero, A., Santos, A., Oturan, M. A., 2018. Removal
668 of Organochlorine Pesticides from Lindane Production Wastes by Electrochemical
669 Oxidation. Environ. Sci. Pollut. Res. (doi: 10.1007/s11356-018-1425-4).

670 Dominguez, C. M., Rodriguez, S., Lorenzo, D., Romero, A., Santos, A., 2016.
671 Degradation of hexachlorocyclohexanes (HCHs) by stable zero valent iron (ZVI)
672 microparticles. Water Air Soil Pollut., 227 (12), 446.

673 Dutchak, S., Shatalov, V., Mantseva, M., Rozovskaya, O., Vulykh, N., Fedyunin, M.,
674 Aas, W., Breivik, K., Mano, S., 2004. Persistent organic pollutants in the
675 environment, status report 3. Cooperative Programme for Monitoring and
676 Evaluation of the Long-Range Transmission of Air Pollutants in Europe.
677 http://www.msceast.org/reps/3_2005.pdf.

678 El-Ghenymy, A., Rodríguez, R. M., Brillas, E., Oturan, N., Oturan, M. A., 2014.
679 Electro-Fenton degradation of the antibiotic sulfanilamide with Pt/carbon-felt and
680 BDD/carbon-felt cells. Kinetics, reaction intermediates, and toxicity assessment.
681 Environ. Sci. Pollut. Res. 21(14), 8368-8378.

682 Fu, H., Quan, X., Liu, Z., Chen, S., 2004. Photoinduced transformation of γ-HCH in the
683 presence of dissolved organic matter and enhanced photoreactive activity of
684 humate-coated α-Fe2O3. Langmuir, 20 (12), 4867-4873.

685 Garcia-Segura, S., Keller, J., Brillas, E., Radjenovic, J., 2015. Removal of organic
686 contaminants from secondary effluent byanodic oxidation with a boron-doped
687 diamond anode astertiary treatment. J. Hazard. Mater. 283, 551–557.

688 Garcia-Segura, S., Ocon, J. D., Chong, M. N., 2018. Electrochemical oxidation
689 remediation of real wastewater effluents-A review. Process Saf Environ Prot, 113,
690 48-67.

691 Grannas, A. M., Cory, R. M., Miller, P. L., Chin, Y., McKnight, D. M., 2012. The role
692 of dissolved organic matter in arctic surface waters in the photolysis of
693 hexachlorobenzene and lindane. J. Geophys. Res.: Biogeosciences 117 (G1).

694 Heusinkveld, H. J., Thomas, G. O, Lamot, I., Van den Berg, M., Kroese, A. B. A.,
695 Westerink, R. H. S., 2010. Dual actions of lindane (γ-hexachlorocyclohexane) on
696 calcium homeostasis and exocytosis in rat PC12 cells. Toxicol. Appl. Pharmacol.,
697 248, 12-19.

698 Hubler, D. K., Baygents, J. C., Chaplin, B. P., Farrell, J., 2014. Understanding chlorite
699 and chlorate formation associated with hypochlorite generation at boron doped
700 diamond film anodes. J. Electrochem. Soc., 161(12), E182-E189.

701 Joo, S. H. and Zhao, D., 2008. Destruction of lindane and atrazine using stabilized iron
702 nanoparticles under aerobic and anaerobic conditions: Effects of catalyst and
703 stabilizer. Chemosphere, 70 (3), 418-425.

704 Khan, S., Han, C., Khan, H. M., Boccelli, D. L., Dionysiou, D. D., 2017a. Efficient
705 degradation of lindane by visible and simulated solar light-assisted S-TiO
706 2/peroxymonosulfate process: Kinetics and mechanistic investigations. J. Mol.
707 Catal. A: Chem., 428, 9-16.

708 Khan, S., He, X., Khan, H. M., Boccelli, D., Dionysiou, D. D., 2016. Efficient
709 degradation of lindane in aqueous solution by iron (II) and/or UV activated
710 peroxymonosulfate. J. Photochem. Photobiol. A: Chem., 316, 37-43.

711 Khan, S., He, X., Khan, J. A., Khan, H. M., Boccelli, D. L., Dionysiou, D. D., 2017b.
712 Kinetics and mechanism of sulfate radical-and hydroxyl radical-induced
713 degradation of highly chlorinated pesticide lindane in UV/peroxymonosulfate
714 system. Chem. Eng. J., 318, 135-142.

715 Khaydarov, R. A., Khaydarov, R. R., Gapurova, O., 2013. Nano-photocatalysts for the
716 destruction of chloro-organic compounds and bacteria in water. J. Colloid Interface
717 Sci., 406, 105-110.

718 Labiadh, L., Oturan, M. A., Panizza, M., Hamadi, N. B., Ammar, S., 2015. Complete
719 removal of AHPS synthetic dye from water using new electro-Fenton oxidation
720 catalyzed by natural pyrite as heterogeneous catalyst. J. Hazard. Mater., 297, 34-41.

721 Martínez-Huitle, C. A. and Brillas, E., 2009. Decontamination of wastewaters
722 containing synthetic organic dyes by electrochemical methods: a general review.
723 Appl. Catal. B-Environ., 87 (3), 105-145.

724 Martinez-Huitle, C. A. Rodrigo, M. A. Sirés, I. Scialdone, O., 2015. Single and coupled
725 electrochemical processes and reactors for the abatement of organic water
726 pollutants: A critical review. Chem. Rev. 115, 13362-13407.

727 Moreira, F. C., Boaventura, R. A., Brillas, E., Vilar, V. J. (2017). Electrochemical
728 advanced oxidation processes: a review on their application to synthetic and real
729 wastewaters. Appl. Catal. B-Environ., 202, 217-261.

730 Nienow, A. M., Bezares-Cruz, J. C., Poyer, I. C., Hua, I., Jafvert, C. T., 2008. Hydrogen
731 peroxide-assisted UV photodegradation of Lindane. Chemosphere, 72 (11), 1700-
732 1705.

733 Nitoi, I., Oncescu, T., Oancea, P., 2013. Mechanism and kinetic study for the
734 degradation of lindane by photo-Fenton process. J. Industrial Eng. Chem., 19 (1),
735 305-309.

736 Oturan, M. A. and Aaron, J. J., 2014. Advanced oxidation processes in
737 water/wastewater treatment: principles and applications. A review. Crit. Rev.
738 Environ. Sci Technol. 44 (23), 2577-2641.

739 Oturan, M. A., Pimentel, M., Oturan, N., Sirés, I., 2008. Reaction sequence for the
740 mineralization of the short-chain carboxylic acids usually formed upon cleavage of
741 aromatics during electrochemical Fenton treatment. Electrochim. Acta, 54 (2), 173-
742 182.

743 Oturan, N., Wu, J., Zhang, H., Sharma, V. K., Oturan, M. A., 2013. Electrocatalytic
744 destruction of the antibiotic tetracycline in aqueous medium by electrochemical
745 advanced oxidation processes: effect of electrode materials. Appl. Catal. B-
746 Environ., 140-141, 92-97.

747 Panizza, M. and Cerisola, G., 2005. Application of diamond electrodes to
748 electrochemical processes. Electrochim. Acta, 51 (2), 191-199.

749 Panizza, M. and Cerisola, G., 2009. Direct and mediated anodic oxidation of organic
750 pollutants. Chem. Rev. 109, 6541-6569.

751 Peng, L., Deng, D., Guan, M., Fang, X., Zhu, Q., 2015. Remediation HCHs POPs-
752 contaminated soil by activated persulfate technologies: Feasibility, impact of
753 activation methods and mechanistic implications. Separ. Purif. Technol., 150, 215-
754 222.

755 Radjenovic, J. and Sedlak, D. L., 2015. Challenges and opportunities for
756 electrochemical processes as next-generation technologies for the treatment of
757 contaminated water. Environ. Sci. Technol., 49 (19), 11292-11302.

758 Randazzo, S., Scialdone, O., Brillas, E., Sirés, I., 2011. Comparative electrochemical
759 treatments of two chlorinated aliphatic hydrocarbons. Time course of the main
760 reaction by-products. J. Hazard. Mater., 192 (3), 1555-1564.

761 Rodrigo, M. A, Oturan, N., Oturan, M. A., 2014. Electrochemically assisted
762 remediation of pesticides in soils and water: A review. Chemical Reviews 114,
763 8720-8745.

764 Rodrigo, M. A., Michaud, P. A., Duo, I., Panizza, M., Cerisola, G., Comninellis, C.,
765 2001. Oxidation of 4-chlorophenol at boron-doped diamond electrode for
766 wastewater treatment. J. Electrochem. Soc., 148, 60-64

767 Senthilnathan, J. and Philip, L., 2010. Photocatalytic degradation of lindane under UV
768 and visible light using N-doped TiO_2. Chem. Eng. J., 161 (1), 83-92.

769 Sirés, I. and Brillas, E., 2012. Remediation of water pollution caused by pharmaceutical
770 residues based on electrochemical separation and degradation technologies: a
771 review. Environ. Int., 40, 212-229.

772 Sirés, I., Brillas, E., Oturan, M. A., Rodrigo, M. A., Panizza, M., 2014. Electrochemical
773 advanced oxidation processes: today and tomorrow. A review. Environ. Sci. Pollut.
774 Res., 21 (14), 8336-8367.

775 Sopaj, F., Oturan, N., Pinson, J., Podvorica, F. and Oturan, M. A., 2016. Effect of the
776 anode materials on the efficiency of the electro-Fenton process for the
777 mineralization of the antibiotic sulfamethazine. Appl. Catal. B: Environ., 199, 331-
778 341.

779 Ting, D., Steinmaus, C. Perchlorate: human toxicity reference module in earth systems
780 and environmental sciences, in: J.O. Nriagu (Ed.), Encyclopedia of Environmental
781 Health, Elsevier Science, London, 2013, pp.364-370.

782 Usman, M., Tascone, O., Faure, P., Hanna, K., 2014. Chemical oxidation of
783 hexachlorocyclohexanes (HCHs) in contaminated soils. Sci. Total Environ., 476,
784 434-439.

785 Van Wijk, D. J., Kroon, S. G. M., Garttener-Arends, I. C. M., 1998. Toxicity of chlorate
786 and chlorite to selected species of algae, bacteria, and fungi. Ecotox. Environ. Safe.
787 40, 206-211.

788 Vasudevan, S. and Oturan, M. A., 2014. Electrochemistry: as cause and cure in water
789 pollution—an overview. Environ. Chem. Lett. 12(1), 97-108.

790 Vijgen, J., Abhilash, P., Li, Y. F., Lal, R., Forter, M., Torres, J., Singh, N., Yunus, M.,
791 Tian, C., Schäffer, A., 2011. Hexachlorocyclohexane (HCH) as new Stockholm
792 Convention POPs - a global perspective on the management of Lindane and its
793 waste isomers. Environ. Sci. Pollut. Res., 18 (2), 152-162.

794 Wacławek, S., Antoš, V., Hrabák, P., Černík, M., 2016. Remediation of
795 hexachlorocyclohexanes by cobalt-mediated activation of peroxymonosulfate.
796 Desalin. Water Treat., 57 (54), 26274-26279.

797 Wang, Z., Peng, P., Huang, W., 2009. Dechlorination of gamma-
798 hexachlorocyclohexane by zero-valent metallic iron. J. Hazard. Mater., 166 (2-3),
799 992-997.

800 World Health Organization, 2004. Lindane in Drinking-water. Background document
801 for development of WHO Guidelines for Drinking-water Quality.

802 Yang, S., Lei, M., Chen, T., Li, X., Liang, Q., Ma, C., 2010. Application of zerovalent
803 iron (Fe(0)) to enhance degradation of HCHs and DDX in soil from a former
804 organochlorine pesticides manufacturing plant. Chemosphere, 79 (7), 727-732.

805 Zinovyev, S. S., Shinkova, N. A., Perosa, A., Tundo, P., 2004. Dechlorination of
806 lindane in the multiphase catalytic reduction system with Pd/C, Pt/C and Raney-Ni.
807 Appl. Catal. B-Environ., 47(1), 27-36.

808

809

810 **Figure captions**

811

812 **Figure 1.** Influence of the anode (Pt, DSA and BDD) and cathode (CF, CS and SS)
813 materials on the concentration decay of lindane (a, b) and TOC removal (c, d) during
814 electrooxidation of 10 mg L^{-1} lindane in 50 mM Na_2SO_4 solution at 8.33 mA cm^{-2} and a
815 natural initial pH of 6.5.

816 **Figure 2.** Effect of different anode (Pt, DSA and BDD) and cathode (CF, CS and SS)
817 materials on the change of Cl^- (a, b) and ClO_3^- (c, d) with electrolysis time during
818 electrooxidation of 10 mg L^{-1} lindane in 50 mM Na_2SO_4 solution at 8.33 mA cm^{-2} and a
819 natural solution pH of 6.5.

820 **Figure 3.** Effect of the different anode (Pt, DSA and BDD) and cathode (CF, CS and
821 SS) materials on the specific energy consumption per unit TOC mass removed with
822 percentage of TOC removal (calculated according to equation (13)) during

electrooxidation of 10 mg L^{-1} lindane in 50 mM Na_2SO_4 solution at 8.33 mA cm^{-2} and natural solution pH of 6.5.

Figure 4. Effect of current density on the normalized concentration decay of lindane with electrolysis time (a) and kinetic analysis assuming a *pseudo*-first order reaction for lindane oxidation (b) using the BDD/CF cell. The inset in Figure 4b shows the relationship between the apparent kinetic constant and the current density. Operating conditions: $[lindane]_0$ = 10 mg L^{-1}, $[Na_2SO_4]$ = 50 mM, $pH_{0,natural}$ = 6.5.

Figure 5. Change of TOC removal kinetics as a function of current density with electrolysis time during electrooxidation of 10 mg L^{-1} (corresponding to initial TOC of 2.45 mg L^{-1}) with the BDD/CF cell. $[Na_2SO_4]$ = 50 mM, $pH_{0,natural}$ = 6.5.

Figure 6. Effect of current density on mineralization current efficiency (MCE%) (a) and energy consumption EC (in kWh per g TOC removed) and (b) calculated according to equations (16) and (13), respectively. $[TOC]_0$ = 2.45 mg L^{-1}, $[Na_2SO_4]$ = 50 mM, $pH_{0,natural}$ = 6.5 and the BDD/CF cell.

Figure 7. Effect of current density on the production and evolution of Cl^- (a) and ClO_3^- (b) ions during electrooxidation of 10 mg L^{-1} lindane in 50 mM Na_2SO_4 solution at natural solution pH of 6.5 using the BDD/CF cell.

Figure 8. Proposed degradation pathway for lindane oxidation by M($^{\bullet}$OH) based on intermediate products generated during electrooxidation.

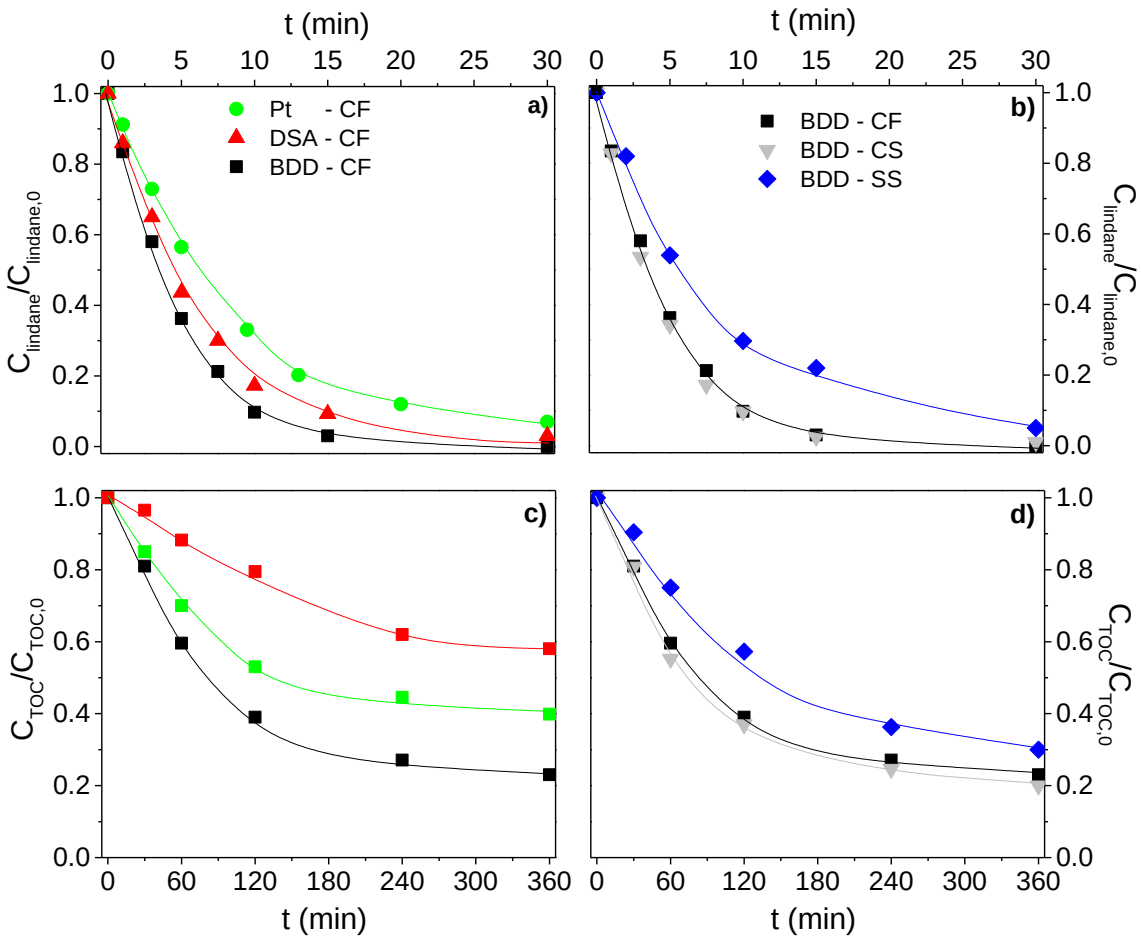

Figure 1. Influence of the anode (Pt, DSA and BDD) and cathode (CF, CS and SS) materials on the concentration decay of lindane (a, b) and TOC removal (c, d) during electrooxidation of 10 mg L^{-1} lindane in 50 mM Na_2SO_4 solution at 8.33 mA cm^{-2} and a natural initial pH of 6.5.

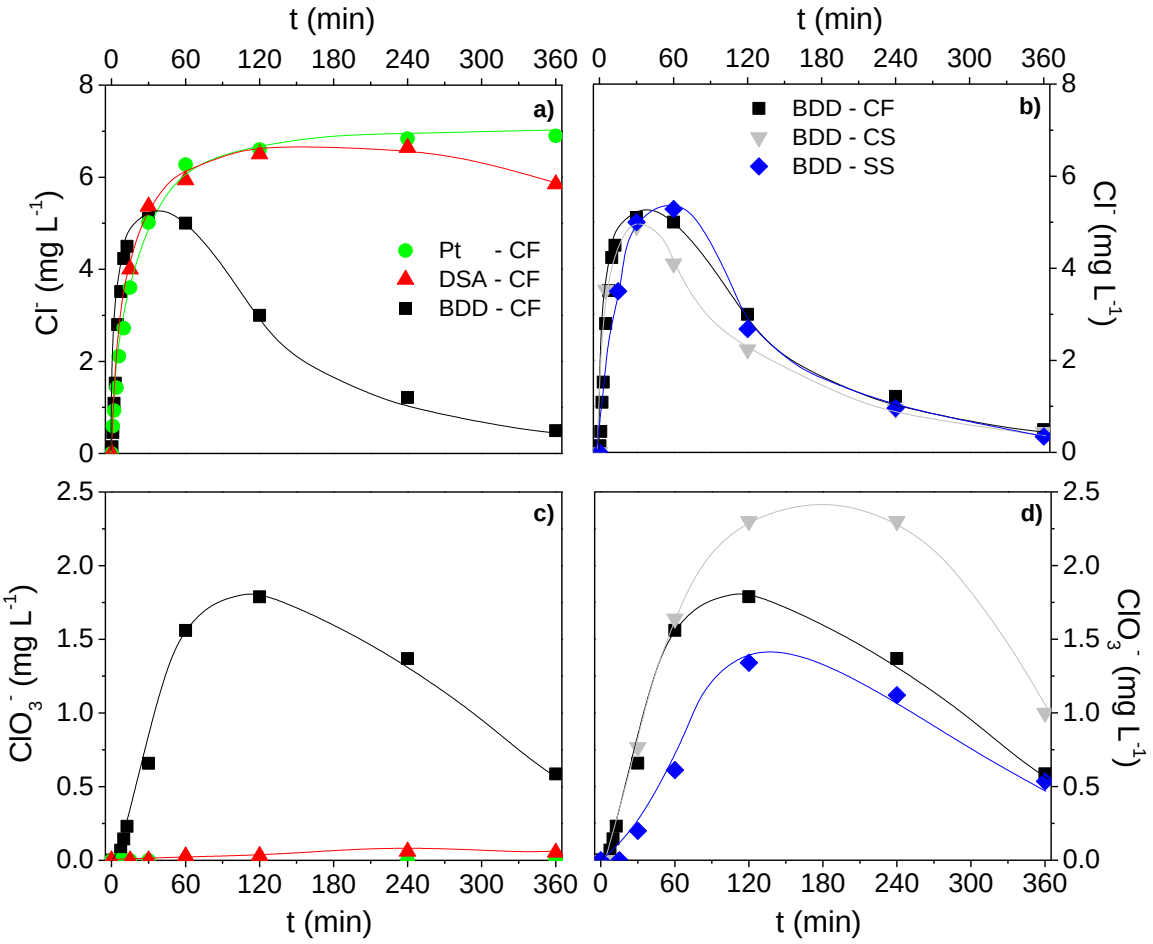

Figure 2. Effect of different anode (Pt, DSA and BDD) and cathode (CF, CS and SS) materials on the change of Cl^- (a, b) and ClO_3^- (c, d) with electrolysis time during electrooxidation of 10 mg L^{-1} lindane in 50 mM Na_2SO_4 solution at 8.33 mA cm^{-2} and a natural solution pH of 6.5.

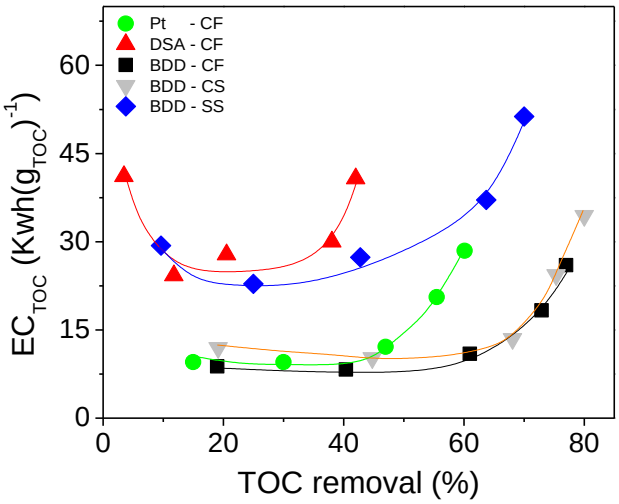

Figure 3. Effect of the different anode (Pt, DSA and BDD) and cathode (CF, CS and SS) materials on the specific energy consumption per unit TOC mass removed with percentage of TOC removal (calculated according to equation (13)) during electrooxidation of 10 mg L^{-1} lindane in 50 mM Na_2SO_4 solution at 8.33 mA cm^{-2} and natural solution pH of 6.5.

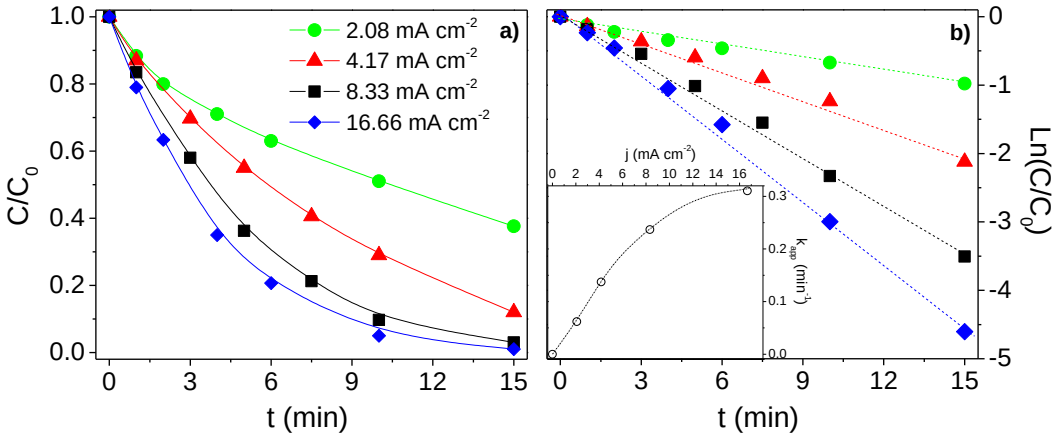

Figure 4. Effect of current density on the normalized concentration decay of lindane with electrolysis time (a) and kinetic analysis assuming a *pseudo*-first order reaction for lindane oxidation (b) using the BDD/CF cell. The inset in Figure 4b shows the relationship between the apparent kinetic constant and the current density. Operating conditions: $[lindane]_0$ = 10 mg L^{-1}, $[Na_2SO_4]$ = 50 mM, $pH_{0,natural}$ = 6.5.

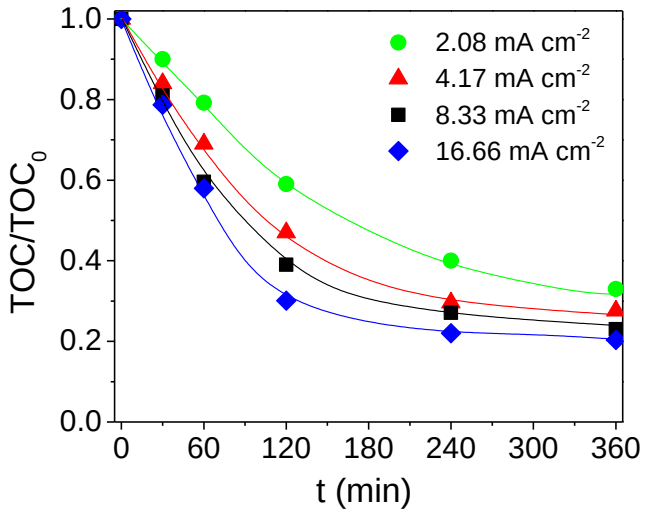

Figure 5. Change of TOC removal kinetics as a function of current density with electrolysis time during electrooxidation of 10 mg L^{-1} (corresponding to initial TOC of 2.45 mg L^{-1}) with the BDD/CF cell. [Na_2SO_4] = 50 mM, $pH_{0,natural}$ = 6.5.

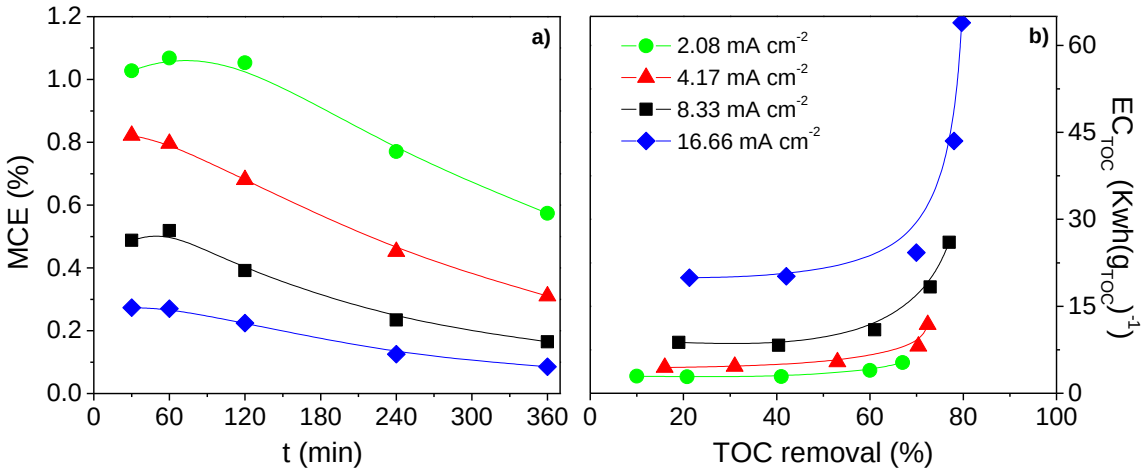

Figure 6. Effect of current density on mineralization current efficiency (MCE%) (a) and energy consumption EC (in kWh per g TOC removed) and (b) calculated according to equations (16) and (13), respectively. $[TOC]_0$ = 2.45 mg L^{-1}, $[Na_2SO_4]$ = 50 mM, $pH_{0,natural}$ = 6.5 and the BDD/CF cell.

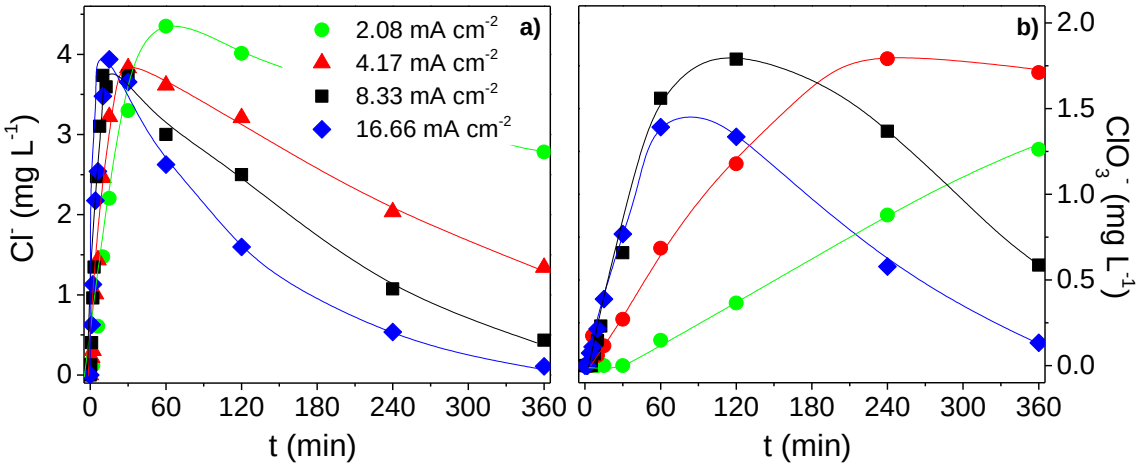

Figure 7. Effect of current density on the production and evolution of Cl^- (a) and ClO_3^- (b) ions during electrooxidation of 10 mg L^{-1} lindane in 50 mM Na_2SO_4 solution at natural solution pH of 6.5 using the BDD/CF cell.

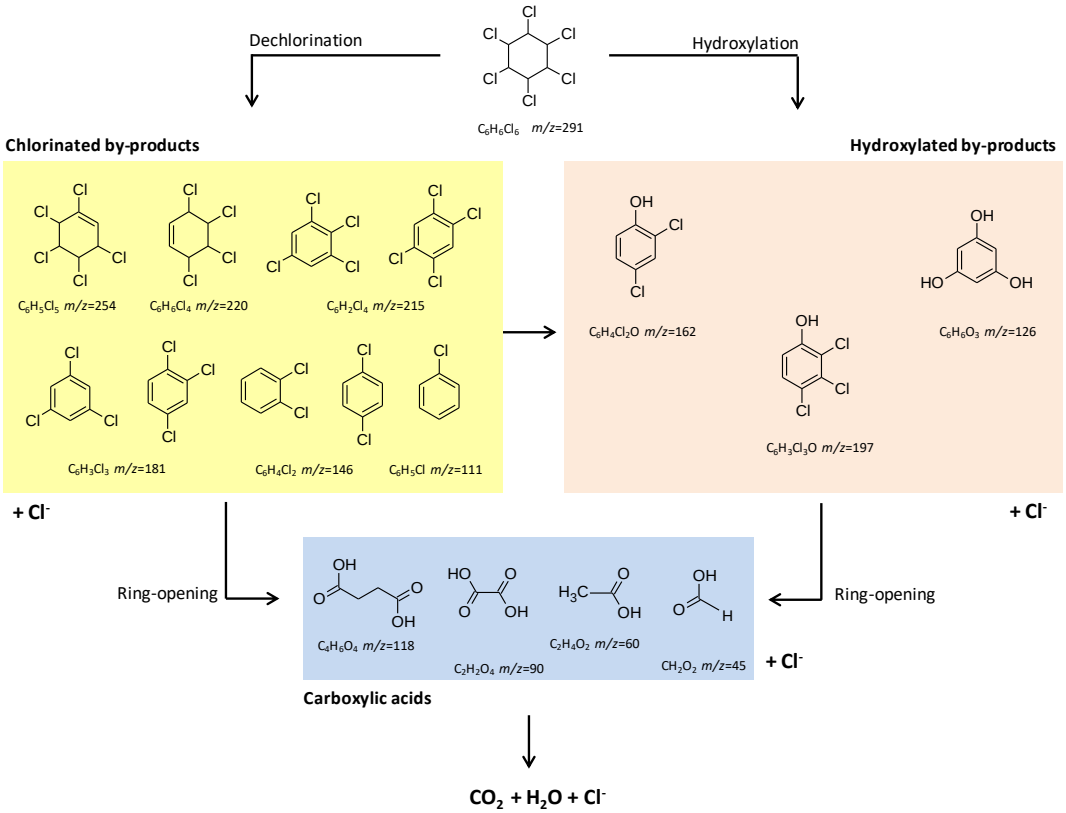

Figure 8. Proposed degradation pathway for lindane oxidation by M(•OH) based on intermediate products generated during electrooxidation.

Supplementary Material

Lindane degradation by electrooxidation process: Effect of electrode materials on oxidation and mineralization kinetics

Carmen M. Dominguez[1,2,*], Nihal Oturan[2], Arturo Romero[1], Aurora Santos[1] and Mehmet A. Oturan[2,*]

[1] Dpto. Ingeniería Química, Facultad de Ciencias Químicas, Universidad Complutense Madrid. Ciudad Universitaria S/N. 28040, Madrid, Spain.

[2] Université Paris-Est, Laboratoire Géomatériaux et Environnement, EA 4508, UPEM, 5 Bd Descartes, 77454 Marne-la-Vallée Cedex 2, France

*E-mails: carmdomi@ucm.es

mehmet.oturan@univ-paris-est.fr

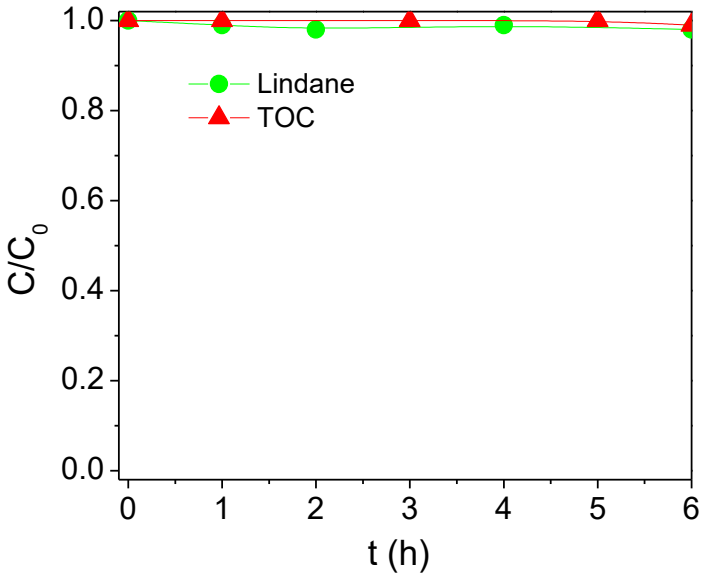

Figure SM 1. Lindane and TOC evolution in the presence of 100 mg L^{-1} H_2O_2.

$[lindane]_0$ = 10 mg L^{-1}, $pH_{0,natural}$ = 6.5, 25 ºC.

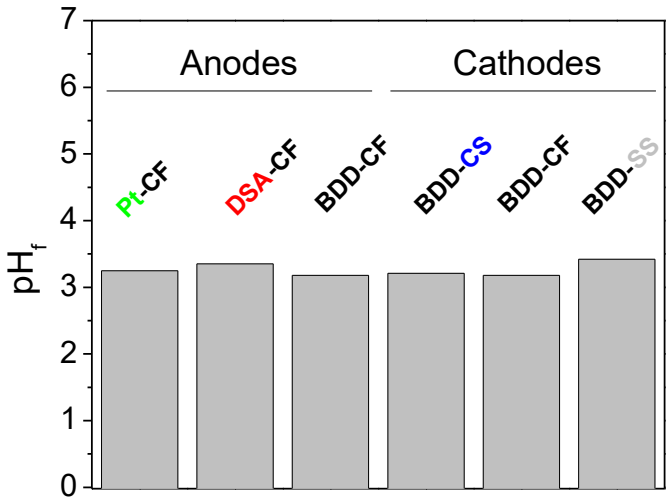

Figure SM 2. Final pH of electrooxidation experiments using different anodic (Pt, DSA and BDD) and cathodic (CS, CF and SS) materials. $[lindane]_0$ = 10 mg L^{-1}, $[Na_2SO_4]_0$ = 50 mM, $pH_{0,natural}$ = 6.5, 25 ºC.

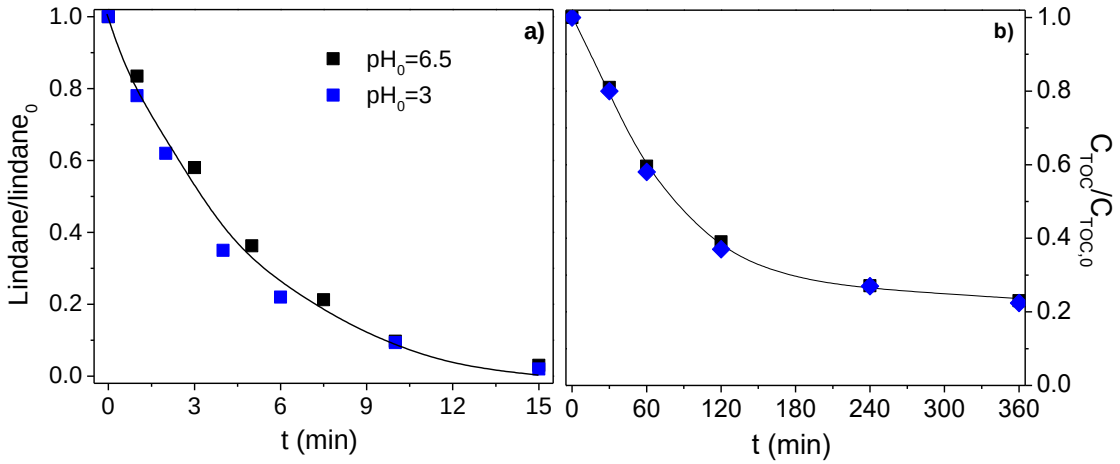

Figure SM 3. Lindane oxidation (a) and mineralization (b) during electrooxidation trials carried out at different initial pHs. $[lindane]_0$ = 10 mg L^{-1}, $[Na_2SO_4]_0$ = 50 mM, 25 ºC.

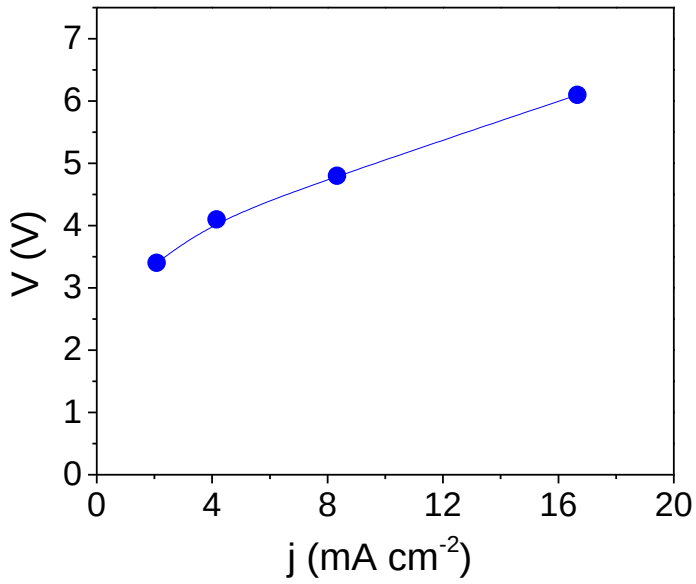

Figure SM 4. Relationship between the potential difference of the cell and the current density during electrooxidation experiments with BDD/CF cell. [lindane] = 10 mg L^{-1}, [Na_2SO_4] = 50 mM, pH_0 = 6.5.

Highlights

- Degradative oxidation/mineralization of organochlorine pesticide lindane
- Best results by using BDD anode / carbon felt cathode cell
- 8.33 mA cm^{-2} appears as effective value for lindane degradation
- Identification of chlorinated, hydroxylated compounds and carboxylic acids
- Transformation of lindane to final mineral end-products: CO_2, H_2O and ClO_4

Graphical Abstract